The Suitability of N_2 to Replace SF_6 in a Triggered Spark-Gap Switch for Pulsed Power Applications

G. Stewart, M.P. Wilson, I.V. Timoshkin, M.J. Given, S.J. MacGregor
Dept. EEE, University of Strathclyde, Glasgow, UK
m.wilson@eee.strath.ac.uk

M.A. Sinclair, K.J. Thomas
AWE Aldermaston, Reading, UK
mark.sinclair@awe.co.uk

***Abstract*-The high dielectric strength of sulphur hexafluoride (SF_6) when compared with other gases, coupled with safety benefits such as non-flammability and non-toxicity, has seen the widespread use of SF_6 for the insulation of switching components. However, SF_6 is now widely recognised as a highly damaging greenhouse gas, and investigations of the switching properties of alternative gases to replace SF_6 within the bounds of existing system topologies are required. In the present paper, a comparative study has been carried out on a triggered spark-gap of type presently deployed in industrial pulsed-power machines, to determine the suitability of nitrogen (N_2) to replace SF_6 as the switching medium, without compromising on functionality. Experiments were performed with fast-rising trigger pulses to minimise the delay time to breakdown and jitter, and three distinct operational regimes have been identified for both gases as the pressure inside the switch is increased. The static breakdown characteristics and upper pressure boundaries of operation have been determined for both gases at a range of dc charging voltages. Measurements of the time to breakdown have shown jitters as low as 1.3 ns when operating in N_2, highlighting the potential of N_2 to replace SF_6 without the need for re-design or replacement of the presently used switch.**

***Index Terms*—Dielectric breakdown, gas insulation, jitter, nitrogen, pulse power system switches, SF_6, spark gaps.**

I. INTRODUCTION

Like gas-insulated switchgear [1] and some transformers [2] and circuit breakers [3] in the power industry, high-voltage switching components throughout the pulsed-power industry are generally insulated with sulphur hexafluoride (SF_6). The high-dielectric strength of SF_6 when compared with other gases, coupled with safety benefits such as non-flammability and non-toxicity, has lead to the widespread use of SF_6 for the insulation of switching components, both internally as a switching medium and externally to prevent flashover and external breakdown events. However, SF_6 is now widely recognised as a highly damaging greenhouse gas, and it looks increasingly likely that legislation may be implemented to force the eventual replacement of SF_6 with a more environmentally friendly alternative.

In the case of future systems where the design phase has yet to be entered, the system could be designed using air as an external insulation, albeit at the expense of a larger-volume system, or oil-insulated to maintain a compact system design, and with switches designed to use an alternative working medium. For existing components and systems however, any legislation forbidding the use of SF_6 could necessitate a complete re-design and replacement of switching components. Considering the case of Mogul-D [4], a 280-tonne pulsed-power machine used for flash X-ray radiography at AWE Aldermaston, this could necessitate the replacement of tens of existing triggered spark-gap switches in the Marx generator section of the pulse-forming network, that have been designed to operate in SF_6. Investigations of the switching properties of alternative gases to replace SF_6 within the bounds of the existing system topology are therefore required.

Triggered spark-gap switches are usually designed in two main forms: mid-plane spark gaps, where the trigger electrode, usually in the form of a ring with a sharp edge to provide field enhancement, is located halfway between two main electrodes; and spark gaps with the trigger electrode located within the earthed main electrode. Such switches are used in synthetic test circuits in the power industry to test high-voltage circuit breakers [5].

Osmokrovic et al. [6] have previously performed tests on both types of spark gap discussed above, and found that the characteristics of the trigger pulse are just as important as spark-gap topology for these types of switch. Measurements were taken for different triggering conditions in vacuum, nitrogen (N_2), and SF_6. Delay times were measured by monitoring the voltage waveform on the trigger electrode, and both the delay time and statistical dispersion of the delay time were found to decrease with increasing rate-of-rise of the trigger pulse in all three switching media. Different electrode materials were tested and the authors concluded that the mid-plane spark gap, with copper electrodes and operating in SF_6, offered superior performance in terms of overall switching characteristics.

The objective of the present work was to compare the switching characteristics of N_2 with those of SF_6, when used as the working medium for a mid-plane triggered spark gap of the type used in AWE's Marx generators, to determine the suitability of N_2 to replace SF_6, preferably without the need for re-design or replacement. The breakdown mechanisms involved in closing of a mid-plane spark-gap switch are discussed in [7].

Important switching characteristics include the rate of voltage collapse between the main electrodes, the delay time to breakdown, and the jitter in the delay time (i.e. the standard deviation of the time to breakdown between repeated switching events). Due to the number of switches involved in AWE's Marx generator systems, and the fact that they are all required to close almost simultaneously to ensure that the

978-0-947649-44-9/09/$26.00

Marx generator produces the optimal output for X-ray pulse generation, the jitter in the delay time to breakdown was investigated as the most significant switching parameter to be compared for each gas.

II. Experimental Arrangement

To provide a baseline to allow comparisons to be made, an existing AWE switch was first characterised using SF_6 as the working medium. Tests were then performed using N_2 as the working medium for comparative purposes. Three types of measurement were conducted to provide information about the switching characteristics in both SF_6 and N_2: the first type involved finding the static breakdown (dc hold-off) voltages associated with breakdown of one half of the symmetrical switch (trigger electrode earthed) at a range of pressures for each gas; the second involved determining triggering regimes and upper boundary pressures of operation; and the third involved determining the jitter in operation at a range of pressures and dc charging voltages. Although the switches are usually oil-immersed at AWE to prevent external breakdown events, lower values of dc charging voltage and trigger pulse magnitude used in the present paper allowed the switch to be operated in atmospheric air.

A schematic diagram of the circuitry for dc hold-off measurements is shown in Fig. 1. The upper main electrode was charged by a 100-kV, Glassman high-voltage dc supply, via a 33-MΩ, oil-immersed, charging resistor chain (R_c). Both the lower main electrode and the central trigger electrode were connected directly to earth for these measurements, and the voltage from the dc supply was increased until self-breakdown of the gas in the gap between the upper main electrode and the trigger electrode occurred. The charging voltages were monitored by a custom-built 10,000:1 dc voltage divider (R_1 & R_2), with the output connected via a BNC connector to a digital multimeter (DMM).

The circuit shown in Fig. 2 was deployed for jitter measurements. The upper main electrode was again charged

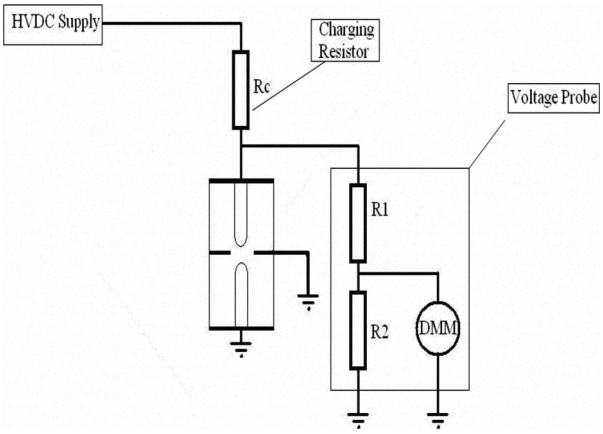

Fig. 1. Schematic diagram of the circuitry used for static breakdown (dc hold-off) measurements.

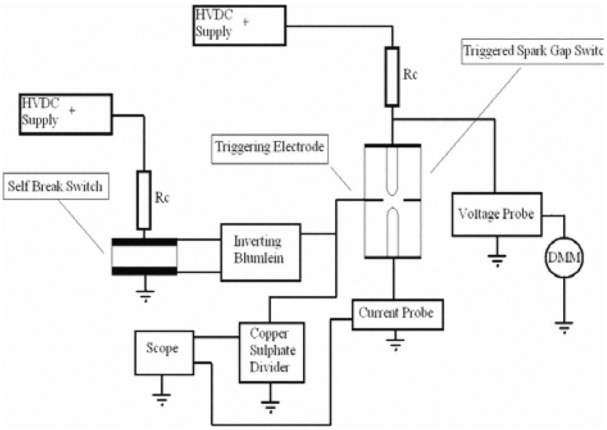

Fig. 2. Schematic diagram of the circuitry used for delay time to breakdown measurements. "Self Break Switch" is PCS(S)-01 self-closing switch; "Copper Sulphate Divider" is DE(LRP)-02 voltage divider; "Current Probe" is DE(CP)-01 resistive current shunt; and "Voltage Probe" is custom-built dc voltage divider.

by the same 100-kV dc supply and charging resistor arrangement, with the charging voltage monitored using the dc voltage divider and multimeter. Trigger pulses were supplied to the central trigger electrode via an inverting, double-Blumlein arrangement. The Blumlein was charged by a 50-kV, Glassman high-voltage dc supply, via another 33 MΩ, oil-immersed, charging resistor chain, and switched via a Samtech Ltd. PCS(S)-01 self-closing switch. The inter-electrode gap on this switch was ~9 mm, giving a self-breakdown voltage of 25 kV when insulated by atmospheric air. The input impedance of the generator is 50 Ω and the output impedance is 200 Ω, meaning that an output pulse of 4x the magnitude of the dc charging voltage can be achieved into an open circuit load. The design and construction of the generator is described in [8].

The trigger pulse voltage waveform was monitored using a Samtech Ltd. DE(LRP)-01 liquid-resistive voltage divider, capable of measuring voltages of up to 300 kV, with a response time of <5 ns. The waveform of the trigger pulse voltage is shown in Fig. 3. The delay time to breakdown was measured as the time difference between the application of

Fig. 3. Trigger pulse voltage waveform from Blumlein. The magnitude is ~75 kV, the pulse width is 125 ns, and the rise-time is 50 ns.

the trigger pulse and current flowing to earth, monitored using a Samtech Ltd. DE(CP)-01 resistive current shunt. The jitter in the delay time was then calculated, following the accepted definition, as the standard deviation of the time to breakdown, with ten measurements taken for each data point. The trigger pulse and current waveforms were monitored using a Tektronix TDS2024, 200 MHz, 2 GS/s, digital storage oscilloscope, and recorded using the built-in flash drive.

III. Experimental Results

A. Static Breakdown Characteristics

The self-breakdown voltages of one half of the spark-gap switch were measured using the experimental arrangement shown in Fig. 1, to determine the relative dc hold-off characteristics of the switch operating in both SF_6 and N_2. The switch was filled to the desired pressure for the gas to be tested, and the dc supply voltage was increased until breakdown occurred, with the charging voltage reading being obtained from the multimeter display. The results displayed in Fig. 4 are for the application of positive dc voltages. Three measurements were taken for each data point, and the results represent the mean values. As expected, the static breakdown voltage (V_s) increases linearly with increasing pressure for both gases, and the gradient of the SF_6 curve in Fig. 4 is much steeper than the N_2 curve, which implies that the switch will need to be operated at higher gas pressures in N_2. At pressures where measurements could be made in both gases, the dc hold-off of the switch when insulated with SF_6 was about 2.2 times greater than that when insulated with N_2.

B. Operational Regimes

On triggered operation of the complete switch in both gases, three distinct operational regimes were found, as indicated by the waveforms shown in Fig. 5 (SF_6) and Fig. 6 (N_2). The waveforms shown in both of these figures were obtained with a constant dc charging voltage of +50 kV applied across the main gap, and constant trigger pulse amplitude of -75 kV. Two diagnostic tools were utilised: the Samtech DE(LRP)-01 voltage probe, to measure the trigger pulse voltage waveform; and the Samtech DE(CP)-01 current shunt, to measure the current flowing through the switch to earth. The full test circuit was as shown in Fig. 2.

Operation was first characterised in SF_6, and the first sharp rise in the current trace in Fig. 5a indicates breakdown occurring between the main electrodes, i.e. switch closure. It is apparent that breakdown has occurred on the rising edge of the trigger pulse, and this type of behaviour was witnessed in low-pressure regimes. As the gas pressure is increased, breakdown occurs after the trigger pulse has reached its peak amplitude, as the time between application of the trigger pulse and switch closure (i.e. the time to breakdown) increases. This behaviour in the intermediate-pressure regime is shown in Fig. 5b. Switching behaviour in high-pressure regimes is illustrated in Fig. 5c, where there is a long delay time between the application of the trigger pulse and closure of the switch,

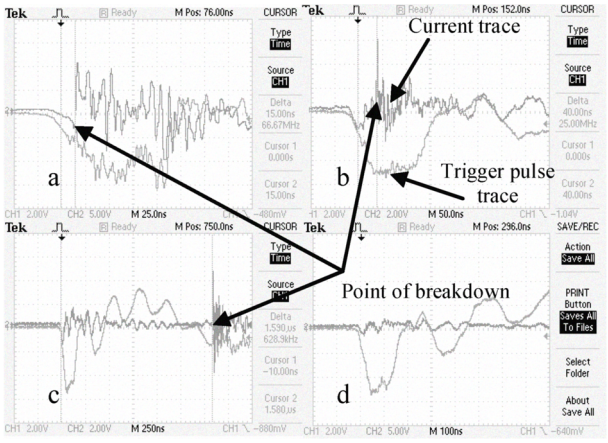

Fig. 5. Typical trigger pulse voltage and current waveforms obtained for switching in SF_6. Fig. 5a: low-pressure regimes; Fig. 5b: intermediate-pressure regimes; Fig. 5c: high-pressure regimes; Fig. 5d: no breakdown of switch. Note the varying time-base to shown the detail in each section of the figure.

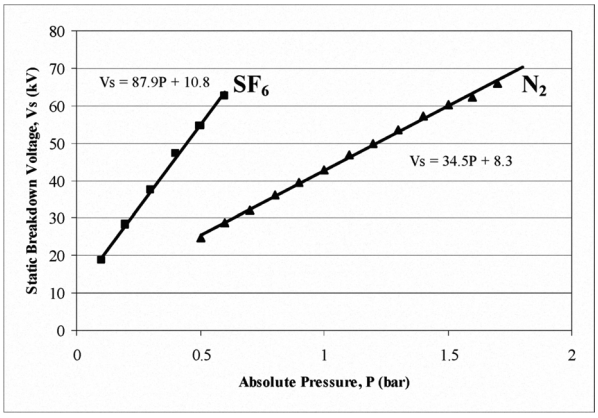

Fig. 4. Static breakdown (dc hold-off) voltages (V_s) versus absolute pressure (P) for breakdown of one half of switch in both SF_6 (closed squares) and N_2 (closed triangles). The equations of the best-fit straight lines are shown for both gases.

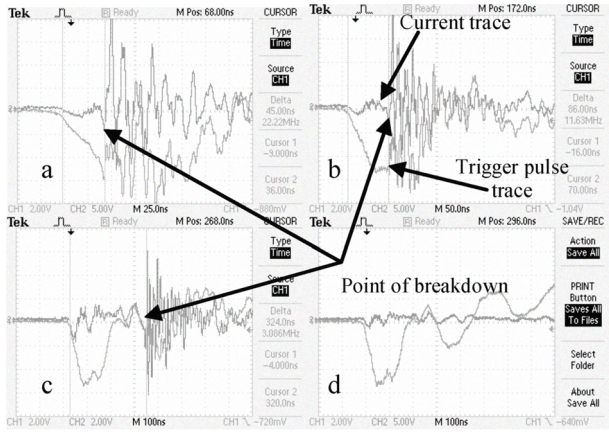

Fig. 6. Typical trigger pulse voltage and current waveforms obtained for switching in N_2. Fig. 6a: low-pressure regimes; Fig. 6b: intermediate-pressure regimes; Fig. 6c: high-pressure regimes; Fig. 6d: no breakdown of switch. Note the varying time-base to shown the detail in each section of the figure.

which is indicated by the transient in the current waveform some 1.5 μs after the trigger pulse begins to rise. This long delay time means that switch closure occurs after the trigger pulse voltage has risen to its peak and fallen to zero, and in this regime the switch is verging on the point of non-operation. With further increase of the gas pressure, the switch fails to close, as indicated in Fig. 5d.

The waveforms displayed in Fig. 6 show that the same three switching regimes were observed when operating in N_2, albeit at higher operational pressures in each regime. The difference in pressure for the three different regimes when operating in N_2 as compared with SF_6 is discussed in section C.

On establishment of these different operating regimes, measurements were performed to find the upper pressure boundary at which the switch could be reliably triggered (switch closure occurring every time triggering is attempted), and the results for a range of dc charging voltages in both SF_6 and N_2 are displayed in Fig. 7. As expected due to the higher-dielectric strength of SF_6, it is apparent that the gradient of the N_2 curve is greater than that of the SF_6 curve, and the upper boundary pressure varies over a range of 1.3 bar in N_2, compared to a range of 0.4 bar in SF_6 for the same range of applied dc charging voltages.

C. *Operational Jitter*

The circuit shown in Fig. 2 was used to measure the time to breakdown, again by analysing the trigger pulse voltage waveform and the current flowing to earth to determine the time difference between application of the trigger pulse and switch closure. For the results reported here, the dc charging voltage was 40 kV, and the results pertaining to static breakdown voltages (Fig. 4) and upper pressure boundaries of operation (Fig. 7) were used to determine a range of operating pressure within which breakdown would occur upon application of each trigger pulse, but without self-breakdown of the gas occurring due to the high dc charging voltage before application of the trigger pulse.

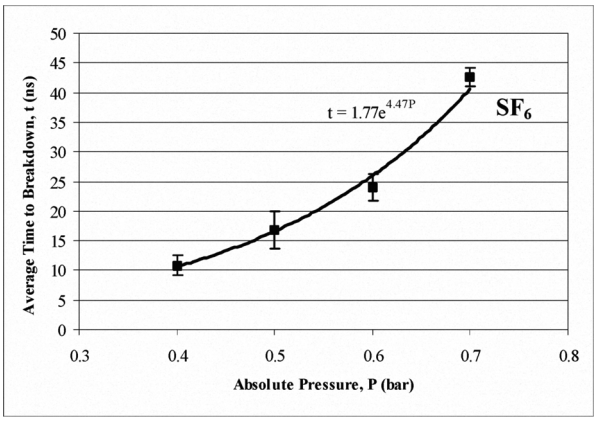

Fig. 8. Average time to breakdown (t) versus absolute pressure (P) for operation in SF_6 with the upper main electrode charged to a dc voltage of 40 kV. An exponential function has been fitted to the data, and the equation is shown.

Ten breakdown events were analysed for each pressure, and the data points shown in Figs. 8 and 9 correspond to the average (mean) time to breakdown. The calculated jitter is represented by the error bars shown in Figs. 8 and 9, and the ± values quoted in the following analysis.

Fig. 8 shows that the average time to breakdown in SF_6 increases exponentially with gas pressure, and varies from 10.8±1.7 ns at 0.4 bar to 42.6±1.6 ns at 0.7 bar. The values of jitter are very low, varying from 1.6-3.0 ns, with the lowest value of jitter being obtained at the highest pressure. The measurement range is limited due to self-closing of the switch at lower pressures, and non-operation at higher pressures.

A similar exponential relationship is observed for switching in N_2, as shown in Fig. 9. The average times to breakdown were longer than those observed in SF_6, partly due to the higher operating pressures required for the same level of dc charging voltage, and the time to breakdown varied from 21.2±2.4 ns at 1.8 bar to 113.2±10.1 ns at 3.2 bar. The values

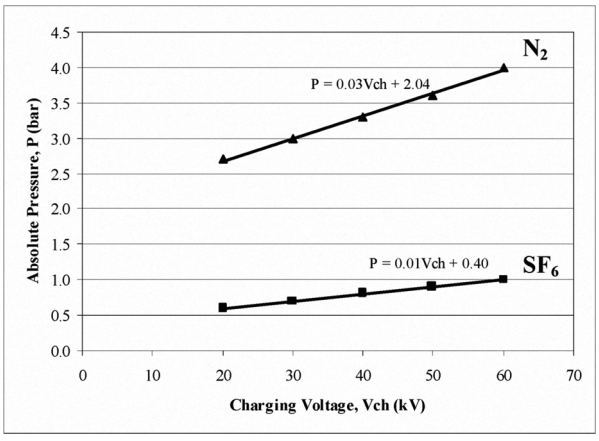

Fig. 7. Boundary pressures of operation (P) versus dc charging voltage (V_{ch}) in both SF_6 (closed squares) and N_2 (closed triangles). The equations of the best-fit straight lines are shown for both gases.

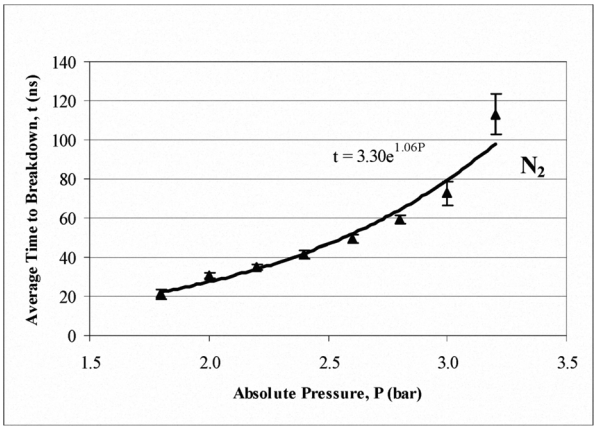

Fig. 9. Average time to breakdown (t) versus absolute pressure (P) for operation in N_2 with the upper main electrode charged to a dc voltage of 40 kV. An exponential function has been fitted to the data, and the equation is shown.

of jitter were again very low, and similar to those observed in SF_6. In the pressure range 1.8-2.8 bar, the jitter values were all below 2.5 ns, with a minimum jitter of 1.3 ns at 2.0 bar. At higher pressures, the jitter increased to 6.1 ns at 3.0 bar and 10.1 ns at 3.2 bar, as the breakdown mechanism varied between inter-mediate pressure and high-pressure switching regimes.

IV. Discussion & Conclusions

A triggered spark-gap switch, of type presently employed in large-scale industrial pulsed-power machines, has been characterised in terms of static breakdown voltages, switching regimes, and jitter in the delay time to breakdown. Tests were conducted on a comparative basis, to determine the potential to replace the now widely recognised greenhouse gas SF_6 with N_2.

For the fast-rising trigger pulses utilised in the study, three distinct operating regimes have been discovered in both gases: low-pressure regimes where switch closure occurred on the rising edge of the trigger pulses; intermediate-pressure regimes where the trigger pulse reached its peak magnitude before switch closure occurred; and high-pressure regimes where switch closure occurred after a significant time delay, after the trigger pulse had reached its peak amplitude and fallen back to zero.

Measurements have shown that while the delay times to breakdown in N_2 are longer than those in SF_6, partly due to the higher operating pressures required for the same level of dc charging voltage, the jitter was very similar in both gases when operating in the correct regime. Jitter levels as low as 1.3 ns were observed in N_2, highlighting the potential to replace SF_6 with N_2 without the need for complete re-design or replacement of the switches, providing that the correct operational regime is utilised by the appropriate choice of gas pressure.

Present environmental pressures mean that this is a significant result towards the replacement of SF_6 with a more environmentally friendly alternative, within the bounds of an existing switch design.

Future work will include analysis of the voltage collapse across the main electrodes at breakdown, and analysis of the relative switching performance of other gases and gas mixtures in the present switch topology.

Acknowledgements

The experimental work was conducted by G. Stewart as an individual undergraduate project during the 4th year of his MEng degree in Electrical & Mechanical Engineering. G. Stewart and M.P. Wilson thank AWE Aldermaston for financial support of the study.

References

[1] S. Okabe, J. Takami, and T. Tsuboi, "Breakdown voltage-time characteristics and insulation testing of gas insulated switchgear," *IEEE Trans. Dielectr. Electr. Insul.*, vol. 15 (3), pp. 741-748, 2008.

[2] K. Hiraishi, Y. Uwano, K. Shirakura, Y. Gotanda, M. Higaki, K. Endoo, M. Horikoshi, K. Mizuno, H. Hora, "Development and practical operation of perfluorocarbon immersed 275kV transformers with compressed SF_6 gas insulation," *IEEE Trans. Power Del.*, vol. 10 (2), pp. 880-888, 1995.

[3] F. Buret, A. Beroual, "SF_6 dielectric behaviour in a high voltage circuit breaker at low temperature under lightning impulses," *IEEE Trans. Power Del.*, vol. 11 (1), pp. 267-273, 1996.

[4] A. Stevens and M. Sinclair, "Mogul-D Marx generator upgrade and predicted output," *IEE Pulsed Power Symposium 2005*, pp. 22/1-3, 2005.

[5] P. Osmokrovic, N. Arsic, Z. Lazarevic, and D. Kusic, "Numerical and experimental design of three-electrode spark gap," *IEEE Trans. Power Del.*, vol. 9 (3), pp. 1444-1450, 1994.

[6] P. Osmokrovic, N. Arsic, Z. Lazarevic, and N. Kartalovic, "Triggered vacuum and gas spark gaps," *IEEE Trans. Power Del.*, vol. 11 (2), pp. 858-864, 1996.

[7] H. Tang and V. Scuka, "The breakdown mechanism of a mid-plane triggered spark gap trigatron," *IEEE Trans. Dielectr. Electr. Insul.*, vol. 3 (6), pp. 843-848, 1996.

[8] I.C. Somerville, S.J. MacGregor, and O. Farish, "An efficient stacked-Blumlein HV pulse generator," *Meas. Sci. Technol.*, vol. 1 (9), pp. 865-868, 1990.